Environmental Science and Pollution Research (2023) 30:21313–21325
https://doi.org/10.1007/s11356-022-23715-0

RESEARCH ARTICLE

Important revelations of different degrees of COVID-19 lockdown on improving regional air quality: a case study of Shijiazhuang, China

Yanan Guan[1,2] · Ying Shen[1] · Xinyue Liu[1] · Xuejiao Liu[1] · Jing Chen[3] · Dong Li[4] · Man Xu[4] · Litao Wang[1,2] · Erhong Duan[1,2] · Li'an Hou[5] · Jing Han[1,2]

Received: 5 September 2022 / Accepted: 14 October 2022 / Published online: 21 October 2022

Abstract

To control the spread of COVID-19, Shijiazhuang implemented two lockdowns of different magnitudes in 2020 (lockdown I) and 2021 (lockdown II). We analyzed the changes in air quality index (AQI), $PM_{2.5}$, O_3, and VOCs during the two lockdowns and the same period in 2019 and quantified the effects of anthropogenic sources during the lockdowns. The results show that AQI decreased by 13.2% and 32.4%, and $PM_{2.5}$ concentrations decreased by 12.9% and 42.4% during lockdown I and lockdown II, respectively, due to the decrease in urban traffic mobility and industrial activity levels. However, the sudden and unreasonable emission reductions led to an increase in O_3 concentrations by 160.6% and 108.4%, respectively, during the lockdown period. To explore the causes of the O_3 surge, the major precursors NO_x and VOCs were studied separately, and the main VOCs species affecting ozone formation during the lockdown period and the source variation of VOCs were identified, and it is important to note that the relationship between diurnal variation characteristics of VOCs and cooking became apparent during the lockdown period. These findings suggest that regional air quality can be improved by limiting production, but attention should be paid to the surge of O_3 caused by unreasonable emission reductions, clarifying the control priorities for urban O_3 management.

Keywords COVID-19 · Lockdown · Air quality index · $PM_{2.5}$ · O_3 · VOCs

Introduction

Since COVID-19 was first reported in Wuhan, China, it has been spreading around the world for more than 2 years. Different countries have taken different measures to control the spread of the virus, and a complete lockdown measure is an effective way to comprehensively control the virus. At the same time, the COVID-19 lockdown has unexpectedly reduced pollutant emissions from anthropogenic sources and improved air quality. Under the lockdown measures such as restrictions on industrial activities, transport and travel (Lal et al. 2020), NO_2, NO, and CO concentrations in Lyon were reduced by 67%, 78%, and 62%, respectively, compared to the normal situation (Sbai et al. 2021). In Delhi, the ban on almost all industrial activities and mass transportation resulted in reductions in PM_{10} and $PM_{2.5}$ which were as high as approximately 60% and 39%, respectively, under the nationwide lockdown measures in India, compared to the pre-lockdown phase (Mahato et al. 2020). Furthermore, compared to pre-pandemic levels, NO_2 concentration has been reduced by 25.5% due to non-essential business closures in the USA (Berman and Ebisu 2020). Wuhan, China, the first city in the world to be under strict lockdown, included actions such as quarantining, traffic restrictions, and factory closures (Cui et al. 2020), reducing NO_2, PM_{10}, $PM_{2.5}$, and SO_2 concentrations by 50.6%, 41.2%, 33.1%, and 16.6%, respectively, compared to the pre-lockdown

Responsible Editor: Lotfi Aleya

✉ Jing Han
hgxhjj@163.com

1 School of Environmental Science and Engineering, Hebei University of Science and Technology, Shijiazhuang 050018, China

2 National Joint Local Engineering Research Center for Volatile Organic Compounds and Odorous Pollution Control, Shijiazhuang 050018, China

3 Shijiazhuang City Environmental Meteorological Center, Shijiazhuang 050018, China

4 Shijiazhuang City Environmental Prediction and Forecast Center, Shijiazhuang 050018, China

5 Xi'an High-Tech Institute, Xi'an 710025, Shaanxi, China

period (Sulaymon et al., 2021). In Jiangsu Province, China, the mean change of $PM_{2.5}$ decreased by 18%, and PM_{10} decreased by 19% from pre-COVID to active COVID (Bhatti et al. 2022). The concentrations of major pollutants SO_2, NO_x, $PM_{2.5}$, and Volatile organic compounds (VOCs) in the Yangtze Delta region were reduced by up to 26%, 47%, 46%, and 57% respectively, during the city lockdown period (Li et al. 2020). NO_x emissions were reduced by 36% over China, compared to the emissions before the outbreak (Feng et al. 2020), and the National Aeronautics and Space Administration (NASA) has published satellite images of the massive reduction in NO_2 over China due to the economic slowdown and reduced human activities (NASA 2020).

Although the concentrations of NO_2, NO, PM_{10}, $PM_{2.5}$, and SO_2 decreased due to the implementation of epidemic control measures, O_3 concentrations increased during the lockdown. Compared to the same period in 2017–2019, the daily O_3 mean concentrations increased at urban stations by 24% in Nice, 14% in Rome, 27% in Turin, 2.4% in Valencia, and 36% in Wuhan during the lockdown in 2020 (Sicard et al. 2020). Similarly, O_3 contents in the industrialized Gujarat state in western India increased by 16–48%, compared to the pre-lockdown (Selvam et al. 2020). This phenomenon is mainly due to stable HCHO concentrations in urban areas, which provides sufficient fuel for tropospheric O_3 generation, especially when there is not enough NO to consume O_3 through the titration effect (Pei et al. 2020).

Shijiazhuang, the capital city of Hebei province, is suffering from severe air pollution with a ranking of 167th in air quality among 168 cities in China in 2020 (MEP 2021a). It is also one of the cities in China to have imposed two lockdowns since the outbreak of COVID-19. The different control measures during the two lockdown periods provide a valuable opportunity to explore the effect of different measures on air quality. This paper analyzes the trends of the air quality index (AQI) and the characteristics of the changes in $PM_{2.5}$ and O_3, the most concerned atmospheric pollutants in China, during the two lockdowns. It then focuses on the causes of O_3 growth in the lockdown, identifying the key species of O_3 formation and changes in the sources of VOCs in the two lockdowns in Shijiazhuang in terms of NO_x and VOCs, the main precursors of O_3. This is important to explore the impact of the ban on air quality and to infer the extent to which regional emission reductions will improve air quality.

Methodology

Study area

Shijiazhuang (SJZ), the third-largest city in the Beijing-Tianjin-Hebei area, is located at 113°30′–115°20′E and 37°27′–38°47′N with an area of 14,464 km^2, as shown in Fig. 1. SJZ consists of 22 districts or counties with a population of 11,023,586 as of November 1, 2020. Petroleum processing, chemical raw material and chemical product manufacturing, pharmaceutical manufacturing, electricity, and construction are the main industries in SJZ (Liu et al. 2018). At the same time, it is also the transportation center of Hebei Province.

For the last 2 years, COVID-19 is raging around the world. In China, Wuhan was the epicenter of the epidemic in 2020. Following a nationwide lockdown, SJZ was less affected by COVID-19, with 29 confirmed cases throughout 2020 (http://www.nhc.gov.cn/). From 25 January to 9 February 2020, SJZ implemented the first-level response to a major public health emergency, which is defined as lockdown I. The lockdown I period includes the Chinese Spring Festival and Lantern Festival. However, on 5 January 2021, SJZ suddenly became the epicenter of the epidemic, with 862 confirmed cases in less than a month (http://www.nhc.gov.cn/). SJZ entered a state of war on January 8 and lifted that state on 29 January. Therefore, the period from 9 to 28 January was defined as lockdown II. During lockdown II, dusty weather was observed from 12 to 16 January, air quality data for these 4 days were removed from this study to truly explore the contribution of the lockdown measures to air quality changes.

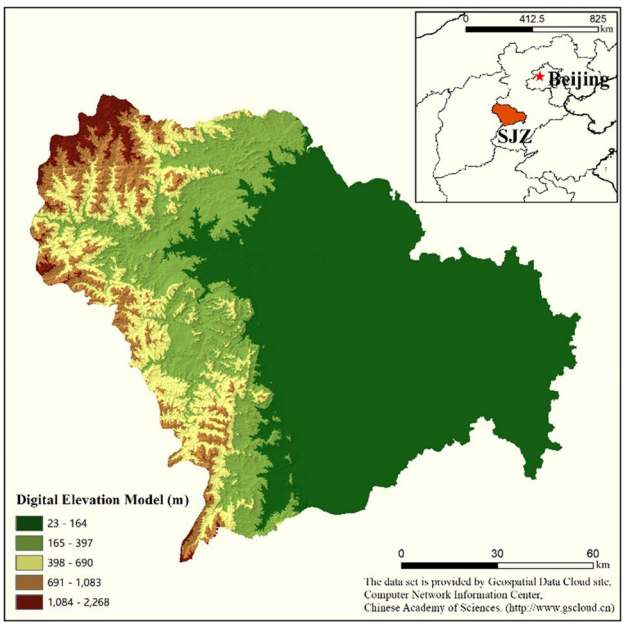

Fig. 1 Location of SJZ

Data source

Hourly concentrations of $PM_{2.5}$ (μg/m^3) and NO_x (μg/m^3), 8-h moving average concentrations of O_3 (μg/m^3), and hourly values of the AQI were obtained from China Environmental Monitoring Station.

Satellite-derived data including tropospheric formaldehyde (HCHO) and tropospheric NO_2 column density were obtained from the Tropospheric Monitoring Instrument (TROPOMI) level-2 retrievals. TROPOMI is a satellite instrument on the Copernicus Sentinel-5 Precursor (S5P) satellite launched by the European Space Agency on 13 October 2017 to monitor air pollution. TROPOMI data was provided on ESA's Sentinels Scientific Data Hub website.

VOC sampling

The monitoring site is located in the Shijiazhuang Ninth High School (38.03°N, 114.28°E), which is part of a mixed educational, residential, and commercial area in the urban area. Online VOC measurement was conducted using AirmOzone Analysis System (ASS) consisting of the AirmoVOC C2-C6 analyzer and AirmoVOC C6-C12 analyzer developed by Chromatotec®. The AirmOzone system uses a flame ionization detector (FID) and monitors a total of 71 VOC species in this study, including 24 alkanes, 12 alkenes, 1 alkyne, 16 aromatics, and 18 halocarbons. The system consists of an internal automatic calibration (AirmoCal) and an external manual calibration. The internal automatic calibration frequency is once a day and the external calibration frequency using VOCs standard gas is once a week, thus ensuring a stable and efficient continuous monitoring of the instrument.

Potential source contribution function

The potential source contribution function (PSCF) is a conditional probability function (Hui et al. 2018), which was applied in this study to locate potential sources of pollution. Using global data provided by the National Center for Environmental Forecasting, the backward trajectories of $PM_{2.5}$ in SJZ during the two lockdowns were calculated in this study with a 24-h backward trajectory height of 100 m.

PSCF can be used to locate the potential source area of the observation points, which is defined as $PSCF_{ij} = m_{ij}/n_{ij}$. Where n_{ij} represents all trajectories in the airflow through the cell grid in the study area, m_{ij} represents the number of pollution trajectories through the grid. In this work, the geographic area covered by the trajectories was divided into an array of $0.1° \times 0.1°$ grid cells, and the $PM_{2.5}$ reference value was set at 75 μg/m^3. The higher PSCF values indicate that the area corresponding to the grid is a potential source area for high concentrations of pollution at the observation site and that the trajectories through this area are a transport pathway that has a significant impact on the observation site.

Since grid cells always have the same PSCF value, it is difficult to distinguish between slightly higher and far higher thresholds (Li et al. 2017). To reduce the effect of small values of n_{ij}, PSCF values are generally multiplied by an arbitrary weighting function W_{ij} to better reflect the uncertainty of these small values (Polissar 1999). W_{ij} is defined in Eq. (1).

$$W_{ij} = \begin{cases} 1.00 & n_{ij} > 80 \\ 0.75 & 80 \geq n_{ij} > 20 \\ 0.42 & 20 \geq n_{ij} > 10 \\ 0.05 & n_{ij} \leq 10 \end{cases} \quad (1)$$

Positive matrix factorization

Positive matrix factorization (PMF) receptor model version 5.0 is developed by the US EPA and used for source analysis of VOCs in SJZ in this study. The PMF model is based on the fundamental principle of mass conservation to identify and apportion source contributions from a given data matrix using Eq. (2) (Assan et al. 2018; Guan et al. 2020; Paatero and Tapper 1994).

$$X_{ij} = \sum_{k=1}^{p} g_{ik} f_{kj} + e_{ij} \quad (2)$$

where X_{ij} represents the VOC concentration matrix with i number of samples and j number of measured VOCs, which are resolved by the PMF to provide p number of possible source factors with the source profile f of each source and mass g contributed by each factor to each sample, leaving the residuals e for each sample (Sarkar et al. 2017). To determine the solution, the minimum value Q is calculated from Eq. (3) (Paatero and Tapper 1994):

$$Q = \sum_{i=1}^{m} \sum_{k=1}^{n} \left[\frac{x_{ij} - \sum_{k=1}^{p} g_{ik} f_{kj}}{u_{ij}} \right] \quad (3)$$

where Q is the object function and a critical parameter for PMF, m and n are sample and species numbers. The uncertainties (Unc) were calculated following the US EPA recommended method as follows: (1) if the concentration values were below or equal to the MDL, their uncertainty was calculated using the following equation: $Unc = 5/6 \times MDL$; (2) if the concentration values were greater than the MDL, the calculation used was: $Unc = [(Error\ fraction \times concentration)^2 + (MDL)^2]^{1/2}$ (Polissar et al. 1998; Reff et al. 2007).

The PMF model was run ranging from 4 to 10 factor numbers to determine the best solution for this study, consistent with the chemical environment in the lockdown of SJZ. The six-factor solution was considered to be the best solution for

this dataset based on the constraints imposed by the Q/Q_{exp} theoretical ratio, the physical likelihood of each factor, and the rotational ambiguity of the solution.

Air quality index

The AQI is a comprehensive pollutant evaluation index that allows for a comprehensive assessment of air quality. According to the Technical Regulation on Ambient Air Quality Index of China, AQI levels are divided into six classes, as shown in Table 1. The AQI is calculated as the maximum value of the air quality sub-index for all air pollutants. Table 2 shows the corresponding air pollution sub-index levels and the corresponding air pollutant concentrations. Six major air pollutants (SO_2, NO_2, PM_{10}, CO, O_3, and $PM_{2.5}$) are selected; their concentrations are grouped into six different categories based on concentration breakpoints. In Table 2, 24-h refers to 24-h average, and 8-h refers to 8-h average. *IAQI* values can be calculated from Eq. (4) by linear interpolation of the reference scale values given in Table 2:

$$IAQIp = \frac{PI_{high} - PI_{low}}{BP_{high} - BP_{low}} \times \left(C_p - BP_{low}\right) + I_{low} \quad (4)$$

Table 1 Air quality index and levels

AQI value	Level
0 ~ 50	Excellent
51 ~ 100	Good
101 ~ 150	Mild pollution
151 ~ 200	Medium pollution
201 ~ 300	Heavy pollution
>300	Serious pollution

where *IAQIp* refers to the air pollution sub-index for pollutant *p*; *Cp* represents the integer concentration of pollutant *p*; BP_{high} represents the breaking point greater than or equal to *Cp*; BP_{low} represents the breaking point less than or equal to *Cp*; PI_{high} refers to the air pollution sub-index corresponding to BP_{high}; and PI_{low} refers to the air pollution sub-index corresponding to BP_{low}. Finally, the *AQI* is calculated as the maximum value of the air pollution sub-indices for all air pollutants, and the air pollutant with the maximum value is identified as the primary pollutant.

Results and discussion

Characteristics of the changes in air quality and AQI

Figure 2 shows the changes in AQI and the proportion of each level during the two lockdowns and from 10 to 25 January 2019 (defined as the same period in 2019). Compared to the same period in 2019, the air pollution levels under the COVID-19 lockdowns decreased significantly, with a 13.2% decrease in AQI for lockdown I and a 32.4% decrease for lockdown II. In terms of the changes in AQI levels, there were 4 days of serious pollution and 1 day of heavy pollution during the same period in 2019, no serious pollution in either lockdown, 6 days of heavy pollution in lockdown I, and 2 days of heavy pollution in lockdown II. In terms of the number of mild and moderate pollution days, the three periods were similar. There were no excellent days in the same period in 2019, and lockdown I and lockdown II had 1 and 2 additional days, respectively. Overall, the improvement in air quality under the lockdown was mainly reflected in the decrease in the number of serious pollution days and the

Table 2 Air quality sub-index levels and their corresponding air pollutant concentrations

Air quality sub-index	Air pollutant concentrations(μg/m^3)									
	SO_2 24-h	SO_2 1-h[a]	NO_2 24-h	NO_2 1-h[a]	PM_{10} 24-h	CO 24-h	CO 1-h[a]	O_3 1-h	O_3 8-h	$PM_{2.5}$ 24-h
0	0	0	0	0	0	0	0	0	0	0
50	50	150	40	100	50	2000	5000	160	100	35
100	150	500	80	200	150	4000	10,000	200	160	75
150	475	650	180	700	250	14,000	35,000	300	215	115
200	800	800	280	1200	350	24,000	60,000	400	265	150
300	1600	[b]	565	2340	420	36,000	90,000	800	800	250
400	2100	[b]	750	3090	500	48,000	120,000	1000	[c]	350
500	2620	[b]	940	3840	600	60,000	150,000	1200	[c]	500

[a]The 1-h-average concentrations of SO_2, NO_2, and CO are just used for real-time reports; the daily concentrations are acquired by 24-h average

[b]The 1-h average concentration of SO_2 will not be included in the calculation of the air quality sub-index, if it is greater than 800 μg/m^3, and the air quality sub-index of SO_2 is reported as 24-h average

[c]The 8-h average concentration of O_3 will not be included in the calculation of air quality sub-index, if it is greater than 800 μg/m^3, and the air quality sub-index of O_3 is reported as 1-h average

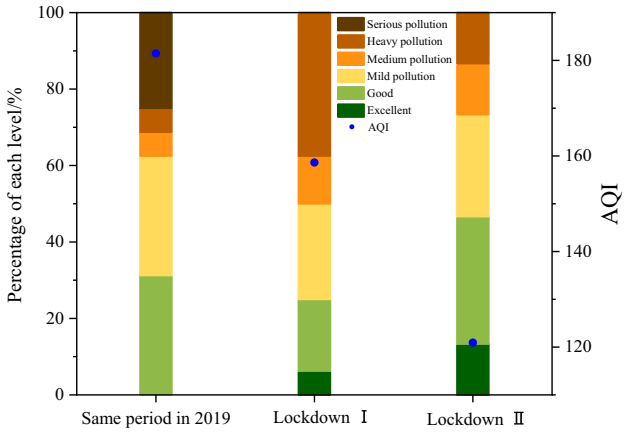

Fig. 2 AQI and air quality degrees in SJZ for the same period in 2019 and the two lockdowns

increase in the number of excellent days. Comparing the two lockdowns, lockdown II was more stringent and had better air quality.

Through the calculation of *IAQIp*, the daily primary pollutants in the same period of 2019 were $PM_{2.5}$ with a 100% contribution; lockdown I was $PM_{2.5}$ with a 100% contribution; and lockdown II was $PM_{2.5}$ and PM_{10} with 47% and 53% contributions, respectively. $PM_{2.5}$ was the primary pollutant in SJZ, and the effect of the lockdown on the change of $PM_{2.5}$ concentration will be analyzed in detail below. Meanwhile, O_3, the main pollutant in SJZ in summer, gradually increased during three periods, as the $PM_{2.5}$ concentration decreased. Therefore, the changes of O_3 concentration during the lockdown period will also be discussed below.

Characteristics of the changes in $PM_{2.5}$ concentrations

In terms of individual pollutants, $PM_{2.5}$ has been the primary pollutant in the Beijing-Tianjin-Hebei region. In 2020, the proportion of non-attainment days with $PM_{2.5}$ as the primary pollutant reached 48% (MEP 2021b). Figure 3 (a) shows the trends of $PM_{2.5}$ hourly concentrations at different AQI levels for three periods. On heavy and serious pollution days, the average $PM_{2.5}$ concentration for the same period in 2019 was 286.6 μg/m^3, which decreased by 37.3% to 179.6 μg/m^3 during lockdown I and by 42.7% to 164.3 μg/m^3 during lockdown II. On mild and medium pollution days, the average $PM_{2.5}$ concentrations were relatively similar for the three periods, at 97.3, 109.1, and 106.1 μg/m^3. Compared to the same period in 2019, on good and excellent days, the average $PM_{2.5}$ concentrations in the three periods were 43.8, 53.5 and 34.7 μg/m^3, respectively; a decrease of 20.8% for lockdown II. As shown in Fig. 3 (b), the average $PM_{2.5}$ concentrations decreased by 12.9% and 42.4% for the whole lockdown I and lockdown II periods, respectively, compared with the same period in 2019. In addition, $PM_{2.5}$ concentrations decreased by 33.8% during lockdown II, compared to lockdown I. It can be concluded that the decrease in $PM_{2.5}$ concentrations in the lockdown occurred mainly on days of heavy and severe pollution, that is, the level of heavy and serious pollution decreased.

The significant reduction in $PM_{2.5}$ concentrations was largely due to the implementation of the lockdown measures. During lockdown I, the policy required people to avoid going outside unnecessarily and allowed one person per household per day to go out to work or shop with a transport permit. However, during lockdown II, due to the SJZ outbreak, the policy required all people to implement home

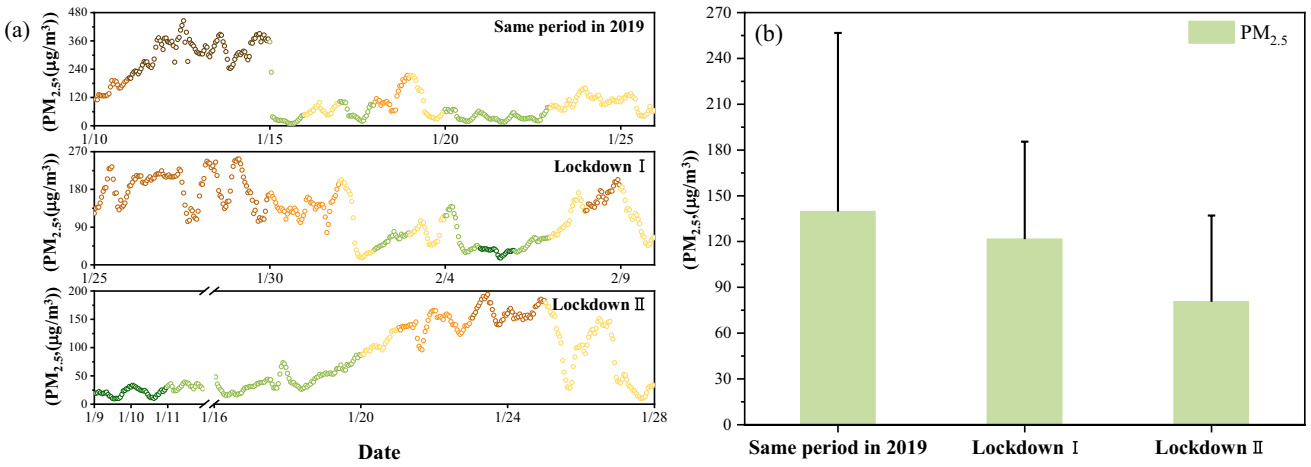

Fig. 3 (a) Temporal variation (different colors correspond to the AQI level colors in Fig. 2) and (b) average concentrations of $PM_{2.5}$ for three periods in SJZ

quarantine, except for medical personnel and those ensuring basic city operations. The difference in policy between lockdown I and lockdown II directly resulted in a significant change in urban traffic mobility. In this study, the intensity of intra-city travel was introduced to characterize urban traffic mobility. The intra-city travel intensities during lockdown I and lockdown II were 1.9 and 1.4, respectively, both significantly lower than 4.0 during the same period in 2019 (http://qianxi.baidu.com). The value during lockdown II was 26.3% lower compared to lockdown I, which proved that lockdown II had fewer traffic sources under the stricter lockdown policy. At the same time, the lockdown policy led to a significant decrease in the level of industrial activity. Compared to the same period in 2019, industrial electricity consumption decreased by 18.8% in lockdown I and 40.0% in lockdown II (SBS 2021). With a 26.2% decrease in industrial electricity use in lockdown II compared to lockdown I, industrial emissions during lockdown II can be estimated to be 26.2% lower than during lockdown I (Li et al. 2021). Moreover, the decrease in $PM_{2.5}$ concentrations during lockdown II was associated with a reduction in firework displays. Lockdown I spanned the Chinese Spring Festival and Lantern Festival, which are two fireworks festivals in China. Fireworks shows have a significant impact on $PM_{2.5}$ concentrations, reaching 50% of $PM_{2.5}$ during the Chinese Spring Festival (Kong et al. 2015; Zhang et al. 2017).

The lockdown policy can only reduce the emissions of local sources but not the contribution of regional transport sources. To clarify the contribution of regional transmission sources to $PM_{2.5}$, we applied the PSCF model, and the results are shown in Fig. 4. With the city of SJZ as the center of the circle, three regions are divided into a radius of 50 km according to the administrative area of SJZ. The area within a radius of 50 km represents the contribution of local sources; the area between 50 and 100 km represents short- and medium-range transport sources; while the other areas correspond to long-range regional transport sources (> 100 km).

From Fig. 4 (a), during the same period in 2019, the highest PSCF values of 0.6–0.7 were found in areas within 50 km, which are industrial areas located in the south and southwest of SJZ. The short and medium distance transmissions between 50 and 100 km were mainly in the western and northeastern areas of SJZ, originating from the eastern part of Yangquan, the southern part of Baoding and the northern part of Xingtai, which were $PM_{2.5}$ potential source areas, with PSCF values mostly between 0.2 and 0.4. When the distance exceeds 100 km, $PM_{2.5}$ was more likely to come from the northern part of Baoding and the northwestern part of Yangquan, with PSCF values between 0.1 and 0.3. As shown in Fig. 4 (b), the high PSCF values were widely distributed within 50 km, indicating that the potential sources of $PM_{2.5}$ during lockdown I were mainly local, especially in the city center, with PSCF values > 0.8. Also, the likelihood of $PM_{2.5}$ from non-industrial areas increased significantly compared to the same period in 2019, indicating a significant increase in pollution from residential emissions during the lockdown. Short- and medium-range transmissions within 50–100 km decreased significantly, with only small transmissions from Yangquan, Xingtai and Baoding, with PSCF values mostly between 0.4 and 0.7. Long-range transmissions over 100 km no longer exist. During lockdown II, SJZ was closed, but the activity level in the surrounding areas was normal. As seen in Fig. 4 (c), the distribution of local sources within 50 km of SJZ was significantly reduced, indicating a low contribution of local sources to $PM_{2.5}$. The higher PSCF values were only distributed near the urban center, with values between 0.5 and 0.8. The transmissions over 50 km were mainly from the east, including the transmissions from the eastern part of SJZ and Hengshui, with PSCF values reaching 0.7.

As can be seen from the discussion above, traffic mobility decreased by 52.5% and industrial activity decreased by 18.8% during lockdown I, compared to the same period in 2019, while both traffic emissions and industrial emissions decreased even more during lockdown II. Compared to lockdown I, urban traffic mobility decreased by 26.3%,

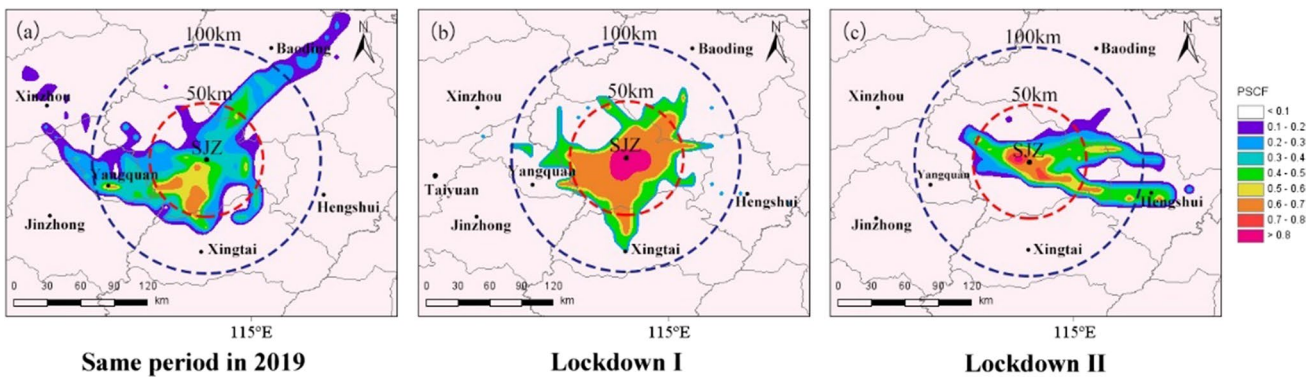

Fig. 4 The potential source contribution function of $PM_{2.5}$ during (a) the same period in 2019, (b) lockdown I, and (c) lockdown II in SJZ

industrial activity decreased by 26.2%, and fireworks emissions were completely reduced in lockdown II, resulting in a 33.8% decrease in $PM_{2.5}$. This suggests that the stricter the lockdown and the lower the level of anthropogenic source activity, the greater the improvement in $PM_{2.5}$.

Characteristics of the changes in O_3 concentrations

From Fig. 5 (a), the average O_3 concentrations on heavy and serious pollution days during these three periods were 8.6, 48.9, and 26.3 μg/m^3, which increased nearly fivefold and twofold during the two lockdowns, respectively. On mild and medium pollution days, the average O_3 concentration for the same period in 2019 was 16.5 μg/m^3, increasing 195.2% to 48.7 μg/m^3 during lockdown I and 116.4% to 35.7 μg/m^3 during lockdown II. On good and excellent days, the average O_3 concentrations for the three periods were 31.8, 49.4, and 45.8 μg/m^3, respectively, with two lockdown periods increased by 55.3% and 44.0%, respectively. Compared with the same period in 2019, the average O_3 concentration increased by 160.6% for the whole lockdown I and 108.4% for lockdown II (Fig. 5(b)), with the increases in O_3 mainly concentrated on heavy and serious polluted days. There are two main reasons for the dramatic increase in O_3 in lockdowns. First, $PM_{2.5}$ concentrations decreased by 27.2% on average, which led to a decrease in the absorption efficiency of hydrogen peroxide radical ($\bullet HO_2$) for $PM_{2.5}$ and an increase in peroxyl radical-mediated O_3 production (Wang et al. 2020). Second, in Fig. 5 (b), the average NO concentration for both lockdowns (3.6 μg/m^3) was more than 10 times lower compared to the same period in 2019 (43.7 μg/m^3), and insufficient NO titration during the lockdowns leads to the accumulation of O_3 (Pei et al. 2020).

To explain the different growths in O_3 in the two lockdowns, we studied the changes in ozone-producing precursors of NO_x ($NO_x = NO + NO_2$) and VOCs, respectively. Due to the occurrence of secondary pollution, from Fig. 5 (b), the mean NO_x concentration (37.0 μg/m^3) was slightly higher in lockdown II than in lockdown I (26.1 μg/m^3), and the mean NO and NO_2 concentrations were 2.6 μg/m^{3}and 24.6 μg/m^3, respectively, in lockdown I and 24.6 μg/m^3 and 30.7 μg/m^3, respectively, in lockdown II. Combining tropospheric NO_2 column density data from TROPOMI satellite (Fig. 6 (a) and (b)), it can be found that local NO_2 column density still decreased during lockdown II compared with lockdown I, especially in the southern part of SJZ where there are industrial areas, and the reduction of NO_x by lockdown was positive.

On the other hand, the mean concentrations of TVOCs were 42.1 and 37.3 ppbv for lockdown I and lockdown II, respectively. We calculated the ozone formation potentials (OFP) during the two lockdowns using the latest indigenous MIR values separately (Zhang et al. 2021), and eight of the top ten species with the largest OFP during the two lockdowns overlapped, as shown in Fig. 6 (e). With almost constant total concentrations for these eight species, the OFP of lockdown II decreased by 11.8%, mainly due to a 46.5% decrease in ethylene concentration. Among the above species, ethylene was the most concentrated species in lockdown I, reaching 6.45 ppbv, while in lockdown II the concentration decreased to 3.45 ppbv. Ethylene is a typical gasoline vehicle emission (Pei et al. 2022; Zhang et al. 2013), and the decrease in its concentration reaffirms the reduction in traffic sources in lockdown II. Propane increased by 45.6% in lockdown II, making it the most abundant species with an increase in OFP of 0.43 ppbv. Trans-2-butene increased more than threefold, corresponding to an increase in OFP

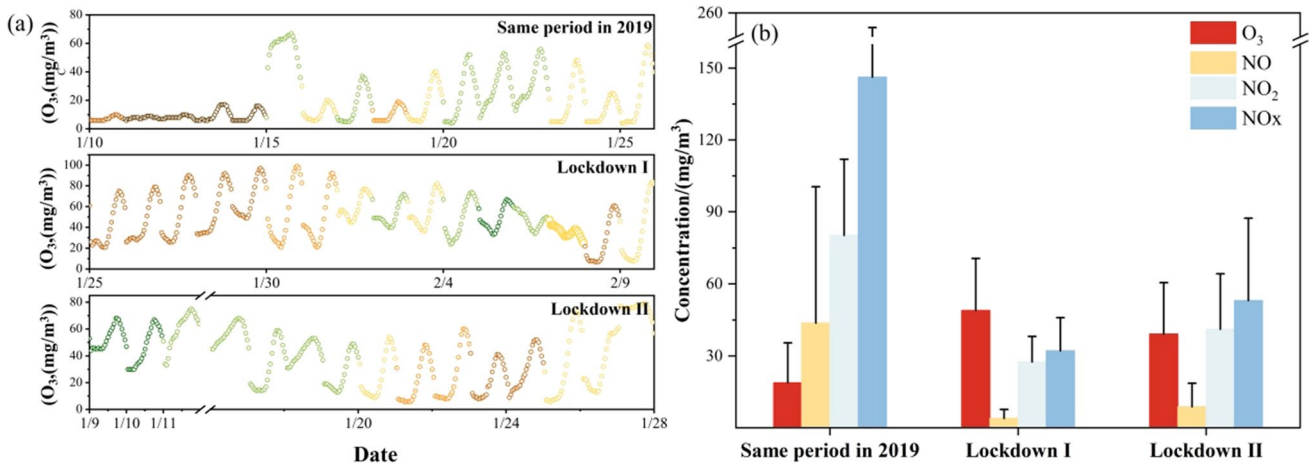

Fig. 5 (a) Temporal variation (different colors correspond to the AQI level colors in Fig. 2) and (b) average concentration of O_3, NO, NO_2, and NO_x for three periods in SJZ

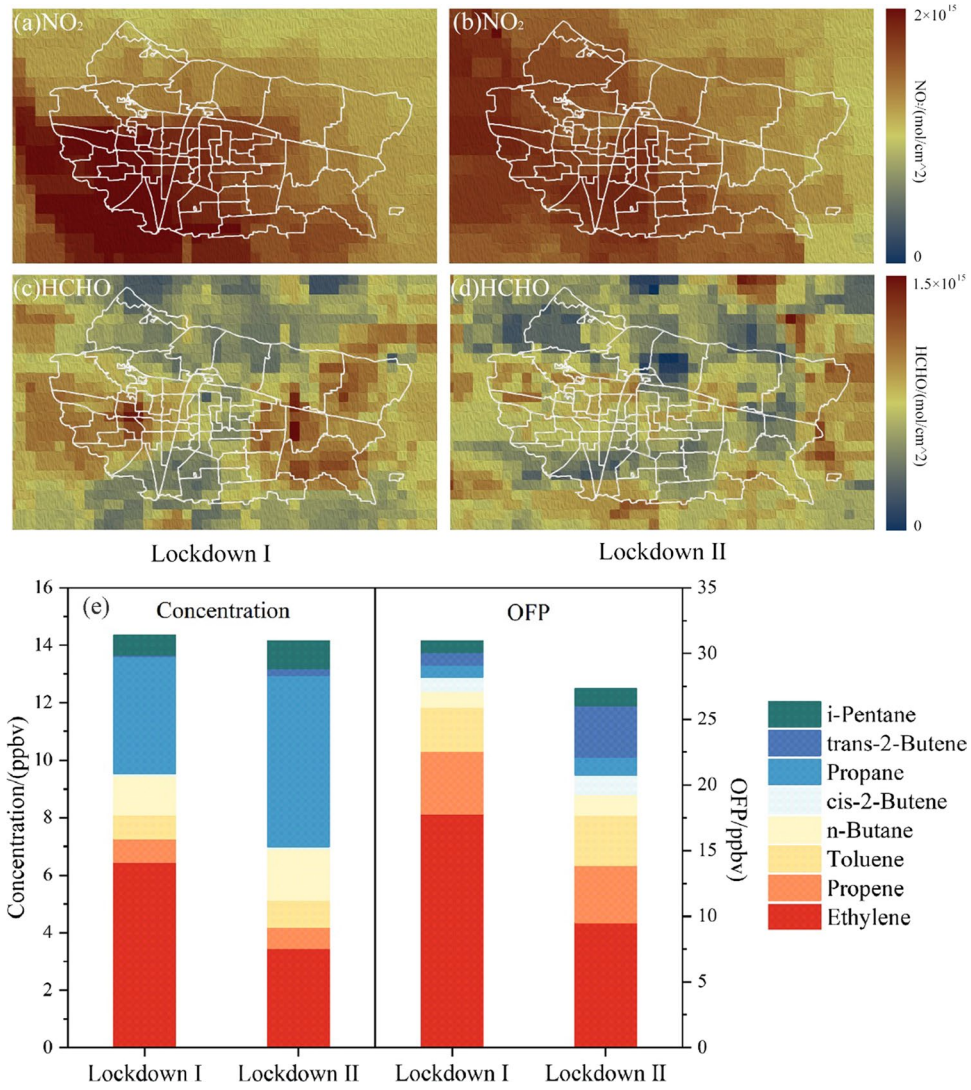

Fig. 6 The satellite image of HCHO and NO_2 in SJZ urban area: (a) NO_2 and (c) HCHO during lockdown I, (b) NO_2 and (d) HCHO during lockdown II and (e) concentrations and OFP of overlapping species in the top ten species ranked by OFP in both lockdowns

of 2.96 ppbv and was one of the main contributors to the increase in OFP in lockdown II. Both propane and trans-2-butene are important species of volatile fuels (Lau et al. 2010), and propane is the main emission associated with liquefied petroleum gas (LPG) (Vega et al. 2000; Xuan et al. 2021). Also, tropospheric formaldehyde (HCHO) column density data were obtained, as shown in Fig. 6 (c) and (d). As the most abundant aldehyde in the atmosphere, HCHO is the most dominant volatile organic compound and pollutant in the troposphere (Peng et al. 2016), and its column concentration variation is positively correlated with energy production and vehicle emissions (Fan et al. 2021), which can be used to assess changes in human activity level. As can be seen in Fig. 6 (c) and (d), the decrease in HCHO column densities was more pronounced in the northern, eastern, and western regions of SJZ during lockdown II compared to lockdown I.

The lower O_3 concentration in lockdown II may be due to a combination of a stronger NO titration reaction and a lower TVOC concentration. But which one dominates? The O_3/NO_x ratio can be used to qualitatively determine the sensitivity of O_3 generation, and a ratio of 15 can be used as a threshold for O_3 generation sensitivity conversion (Tonnesen and Dennis 2000). The O_3/NO_x ratios for both lockdowns and the same period in 2019 were much less than 15, and therefore the SJZ was judged to be a control area for VOCs. This is the same as the result of the previous study (Zhang 2020). Therefore, the difference in O_3 concentrations between the two lockdowns in SJZ was mainly due to the different involvement of VOCs.

VOC profiles during the two lockdowns

From the above discussion, it can be found that VOCs are the key precursor of O_3 generation in SJZ, and its change in the lockdown period can provide ideas for the regional management of O_3. As shown in Fig. 7, alkanes were the most contributing species in both lockdowns, with their share further

increasing by 37.8% in lockdown II, mainly concentrated in light alkanes (C < 6) associated with evaporation emissions of LPG and gasoline (Pei et al. 2022), consistent with the increase in propane described above. In addition, the diurnal variation in alkane concentrations was more severe in lockdown II (14.4 ~ 32.4 ppbv) than in lockdown I (16.2 ~ 19.3 ppbv), suggesting that alkane sources were characterized by heterogeneous temporal variation. Acetylene and aromatics were associated with coal combustion emissions (Barletta et al. 2005; Shi et al. 2015), whose concentrations increased by 13.6% and doubled, respectively, mainly associated with heating during lockdowns. The decrease in VOCs in lockdown II compared to lockdown I was mainly due to an 83.1% reduction in the contribution of halocarbons, which were mainly from industrial processes (Hui et al. 2018).

The VOCs species also produced different daily variation characteristics during the two lockdowns (Fig. 7 (b) and (c)). In lockdown I, all substances showed a clear single-peak distribution with a peak at 9:00 and a trough at 17:00. In contrast, all substances in lockdown II, except alkanes, satisfied a bimodal distribution with two peak times at 9:00 and 21:00 and a trough at 16:00. According to Cheng et al., the types of VOCs detected in Chinese household cooking were alkanes (63.8% ± 4.5%), alkenes (21.9% ± 5.3%) and aromatics (14.3% ± 4.8%) (Cheng et al. 2016), and Chinese home cooking is the most common cooking cuisine in SJZ. Combined with the actual quarantine of people at home during lockdowns, the growth process of alkenes, alkynes, and aromatics overlapped with cooking time, and the contribution of cooking to VOCs may become apparent.

During the lockdown, the sources of VOCs may also change as human activity was greatly restricted. We have analyzed 25 species to identify the contribution of six emission sources to VOCs using PMF (Fig. 8).

In lockdown I, Factor 1 explains the highest contribution of 70.5% for benzene and 53.5% for propane. Benzene is the most abundant VOC species for biomass combustion (Wang et al. 2009), and propane is also one of the major components of non-methane hydrocarbon emissions from biomass stoves in China (Liu et al. 2008; Tsai et al. 2003). Therefore, Factor 1 is identified as biomass burning.

Factor 2 is identified as a traffic source with a contribution of 27.8%, characterized by high contributions from ethane (52.0%) and ethylene (41.7%), which are typical of petrol vehicle emissions. It is worth noting that 30.6% of isoprene is also explained by this factor, and its emissions related to urban transport have been reported previously (Hellén et al. 2012; Sarkar et al. 2017).

Factor 3 is dominated by n-undecane (61.0%), acetylene (58.8%), and some aromatics. Acetylene and aromatics are important indicator species for fossil fuel (Barletta et al. 2005; Shi et al. 2015), therefore, Factor 3 is set as the coal-fired source.

Factor 4 was identified as a biogenic source because it explains more isoprene total mass than any other factor (38.8%).

Factor 5 was determined to be a fuel volatilization source, characterized by a high proportion of C4-C11 n-alkane. Evaporative emissions from China 5 and China 6 gasoline vehicles include C1-C12 alkanes, and C4-C5 alkanes

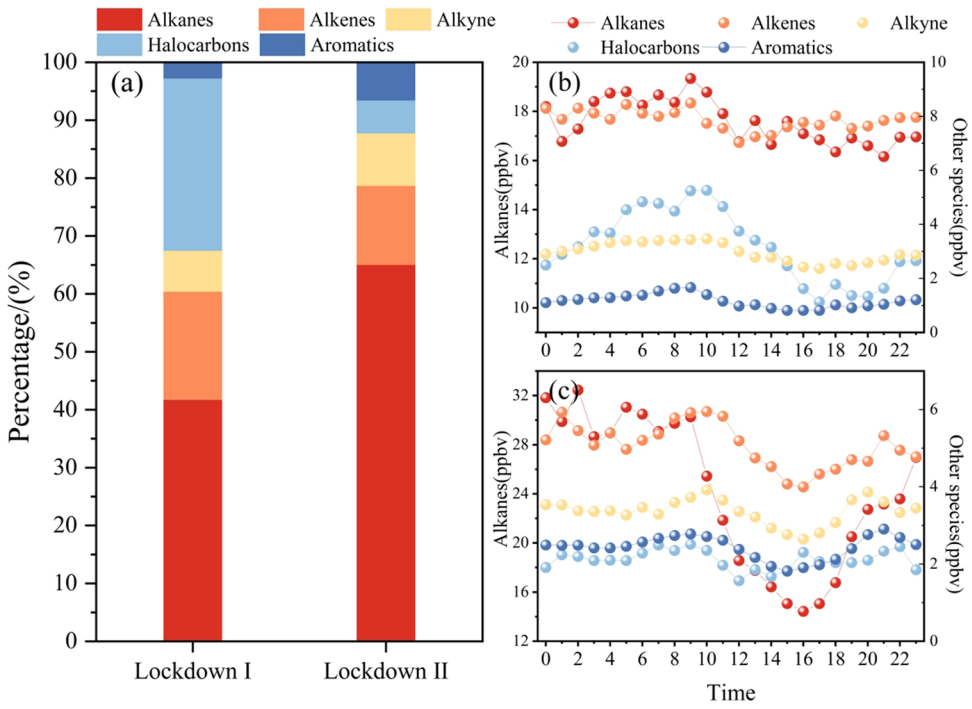

Fig. 7 Changes of VOC species in (a) percentage for both lockdowns and daily concentrations in (b) lockdown I and (c) lockdown II

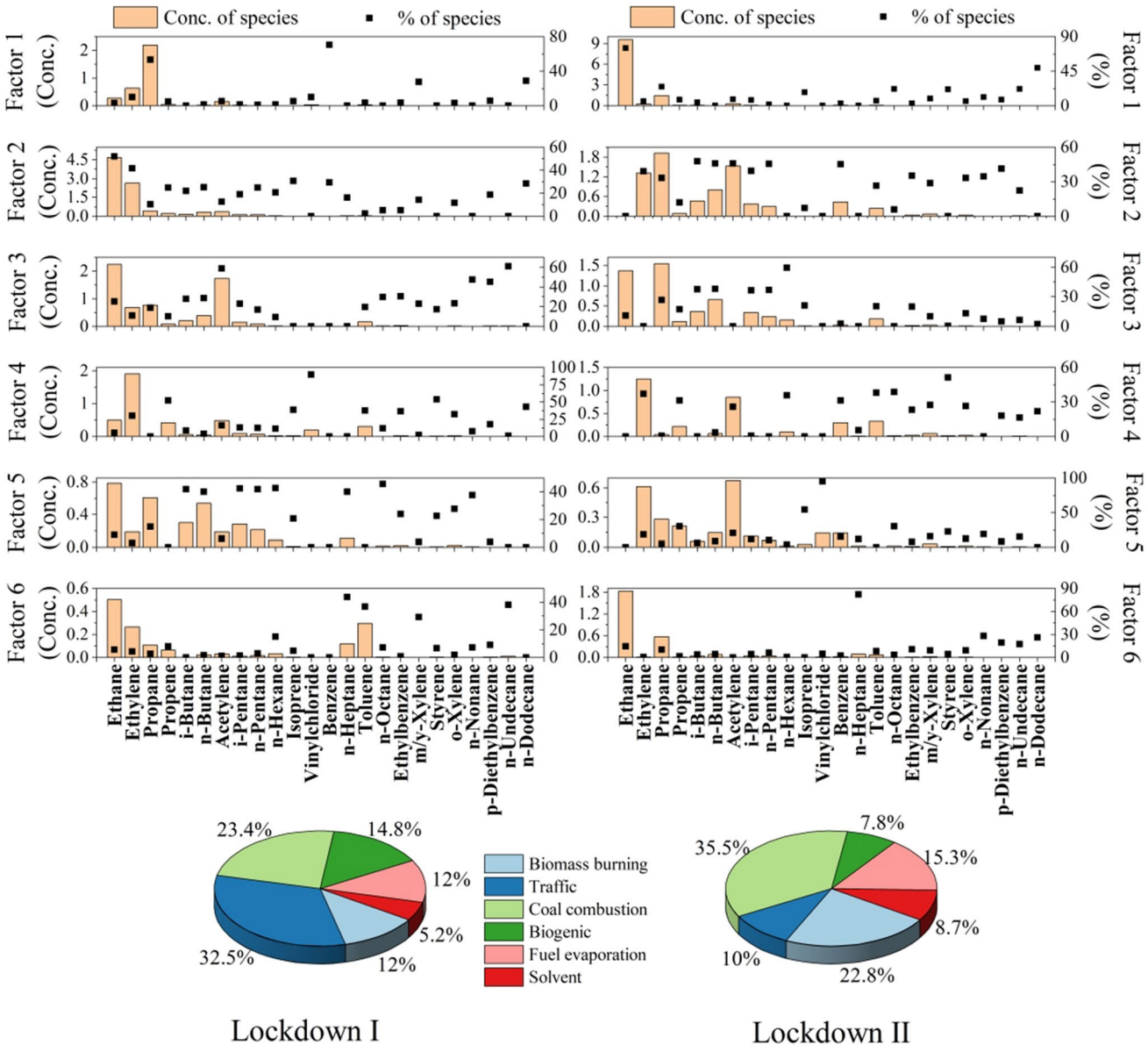

Fig. 8 PMF results for two lockdowns

account for the largest part from China 5 gasoline vehicles' evaporative emissions (Liu et al. 2022), isopentane (42.3%) and n-pentane (41.8%), which are tracers of oil and gas volatilization.

Factor 6 was distinguished by n-heptane (43.8%), n-undecane (38.1%), and toluene (36.9%). Heavy alkanes and aromatics are the dominant VOCs in emissions of the printing industry, and toluene is the most abundant species of the total VOCs emitted from paint applications (Vega et al. 2000; Yuan et al. 2010). Factor 6 was therefore judged to be a solvent source.

In lockdown II, Factor 1 is mainly explained by alkanes and aromatics, including ethane (74.9%), propane (24.6%), toluene (6.4%), and styrene (21.4%), which fit the coal combustion VOC profile and was considered to be the source of coal combustion.

Factor 2 is mainly composed of ethylene (38.9%), acetylene (45.8%), n-butane (47.7%), isobutane (45.7%), benzene (5.3%), and p-diethyl benzene (41.3%). Ethylene and ethyne are important species emitted from biomass open burning (Fang et al. 2017) and have a similar composition to Factor 1 in lockdown I, so Factor 2 is identified as biomass burning.

For Factor 3, high contributing species include n-hexene, n-butane, isobutane, n-pentane and isopentane, which have a similar structural composition to Factor 5 in lockdown I and are identified as fuel volatile sources.

Factor 4 was identified as a traffic source, with high loads of ethylene (36.9%), acetylene (25.7%), benzene (31.4%), and toluene (38.1%), typical of petrol vehicle emissions (Pei et al. 2022; Zhang et al. 2013).

Factor 5 was interpreted as biogenic due to the contribution of 54.4% isoprene.

Factor 6 explains mainly the heavy alkanes, including 82.3% n-heptane, 27.9% n-nonane, and 26.1% n-dodecane, which are major species in printing emissions (Yuan et al. 2010). Therefore, Factor 6 was identified as a solvent source.

The proportion of the sources of VOCs in the two lockdowns is shown in Fig. 7. The ranking of source contributions in lockdown I is traffic source (32.6%) > coal combustion source (23.4%) > biogenic source (14.8%) > fuel evaporation source (12.0%) = biomass burning source (12.0%) > solvent source (5.2%); in lockdown II it is coal combustion source (35.5%) > biogenic source (22.8%) > fuel evaporation source (15.3%) > traffic source (9.9%) > solvent source (8.7%) > biomass burning (7.8%). The reduction of traffic contribution is the main reason for the decrease of VOC concentration in lockdown II, which is consistent with the above conclusion of ethylene reduction. Compared with the two lockdowns, when the restrictions of other sources of VOCs reach a certain limit, reducing the emission from traffic sources is an effective way to reduce the concentration of VOCs.

Conclusion

Since the COVID-19 lockdown significantly limits human activities and was to some extent highly similar to regional abatement activities, the two lockdowns in SJZ provide important insights for improving regional air quality.

The restrictions on human activities caused by the two lockdowns were mainly mirrored in the reduction of urban traffic mobility by 52.5% and 65.0%, respectively, and the reduction of industrial activities by 18.8% and 40.0%, respectively. These restrictions indirectly improved the regional air quality, as reflected by reductions of 13.2% and 32.4% in AQI, and 12.9% and 42.4% in $PM_{2.5}$ concentrations, respectively. Comparing these two lockdowns, it can be concluded that the stricter the lockdown, the greater the air quality improvement, with the decrease in AQI and $PM_{2.5}$ occurring mainly on heavy and serious polluted days and good and excellent days. Meanwhile, the PSCF results show that the $PM_{2.5}$ contribution from local sources dominated, which implies that the focus of improving regional air quality is on the control of local sources.

However, due to unreasonable emission reductions during the lockdown, O_3 concentrations spiked during the two lockdowns, increasing by 160.6% and 108.4%, respectively. First, the decrease in $PM_{2.5}$ concentrations increased the production of O_3 mediated by peroxyl radicals. Second, the average concentrations of NO decreased more than tenfold, which led to a significant reduction in the titration consumption of O_3. The difference in O_3 increase between the two lockdowns was mainly due to an 11.8% decrease in OFP for the major VOC species in lockdown II, especially a 3 ppbv decrease in ethylene concentrations associated with traffic sources. The results of the PMF model again confirmed that the concentration of TVOCs decreased in lockdown II due to a decrease in the contribution of traffic sources. The characteristics and sources of VOCs showed that in lockdown II alkanes increased by 37.8%, especially light alkanes ($C < 6$) associated with LPG, and gasoline evaporative emissions, acetylene, and aromatic hydrocarbons related to coal combustion emissions increased by 13.6% and doubled, respectively, while the contribution of halocarbons from industrial processes decreased by 83.1%. In addition, the diurnal variation characteristics of VOCs in lockdown II, except for alkanes, overlap with the time of household cooking in China. All characteristics were consistent with those of lockdown II, where stringent household policies increased emissions from cooking and coal-fired heating.

The COVID-19 lockdown results suggest that regional air quality can be improved by limiting human activities, but a blind reduction of $PM_{2.5}$ and NO_x may significantly increase O_3 concentrations. Since SJZ is in the VOC control area, future policy should strengthen the control of VOCs, especially for traffic sources. In addition, cooking emissions also need attention.

Author contribution Conceptualization: Dong Li; methodology: Yanan Guan; formal analysis: Ying Shen; software: Xuejiao Liu, Jing Chen; supervision: Erhong Duan; writing — original draft: Xinyue Liu; visualization: Litao Wang; data curation: Man Xu; writing — reviewing and editing: Jing Han; project administration validation: Li'an Hou.

Funding This work was supported by the National Natural Science Foundation of China (Grant number is U20A20130), Natural Science Foundation of Hebei Province (Grant numbers are B2022208020 and B2021208033), Hebei Provincial Department of Science and Technology (Grant number is 22373704D), and Shijiazhuang Science and Technology Bureau (Grant number is 211240233A).

Data availability Hourly concentrations of $PM_{2.5}$ ($\mu g/m^3$) and NO_x ($\mu g/m^3$), 8-h moving average concentrations of O_3 ($\mu g/m^3$) and hourly values of the AQI were obtained from http://106.37.208.233:20035. TROPOMI satellite data was downloaded from (https://scihub.copernicus.eu). Potential source contribution function (PSCF) was done on MeteoInfoMap 2.2.4, available under www.meteothink.org. Positive matrix factorization (PMF) receptor model version 5.0 is available from https://www.epa.gov/air-research/positive-matrix-factorization-model-environmental-data-analyses.

Declarations

Ethical approval Not applicable.

Consent to participate Not applicable.

Consent for publication Not applicable.

Competing interests The authors declare no competing interests.

References

Assan S, Vogel FR, Gros V, Baudic A, Staufer J, Ciais P (2018) Can we separate industrial CH_4 emission sources from atmospheric observations? - A test case for carbon isotopes, PMF and Enhanced APCA. Atmos Environ 187:317–327. https://doi.org/10.1016/j.atmosenv.2018.05.004

Barletta B, Meinardi S, Sherwood Rowland F, Chan C-Y, Wang X, Zou S et al (2005) Volatile organic compounds in 43 Chinese cities. Atmos Environ 39:5979–5990. https://doi.org/10.1016/j.atmosenv.2005.06.029

Berman JD, Ebisu K (2020) Changes in U.S. air pollution during the COVID-19 pandemic. Sci Total Environ 739:139864. https://doi.org/10.1016/j.scitotenv.2020.139864

Bhatti UA, Zeeshan Z, Nizamani MM, Bazai S, Yu Z, Yuan L (2022) Assessing the change of ambient air quality patterns in Jiangsu Province of China pre-to post-COVID-19. Chemosphere 288:132569. https://doi.org/10.1016/j.chemosphere.2021.132569

Cheng S, Wang G, Lang J, Wen W, Wang X, Yao S (2016) Characterization of volatile organic compounds from different cooking emissions. Atmos Environ 145:299–307. https://doi.org/10.1016/j.atmosenv.2016.09.037

Cui Y, Ji D, Maenhaut W, Gao W, Zhang R, Wang Y (2020) Levels and sources of hourly $PM_{2.5}$-related elements during the control period of the COVID-19 pandemic at a rural site between Beijing and Tianjin. Sci Total Environ 744:140840. https://doi.org/10.1016/j.scitotenv.2020.140840

Fan J, Ju T, Wang Q, Gao H, Huang R, Duan J (2021) Spatiotemporal variations and potential sources of tropospheric formaldehyde over eastern China based on OMI satellite data. Atmospheric Pollut Res 12:272–285. https://doi.org/10.1016/j.apr.2020.09.011

Fang Z, Deng W, Zhang Y, Ding X, Tang M, Liu T et al (2017) Open burning of rice, corn and wheat straws: primary emissions, photochemical aging, and secondary organic aerosol formation. Atmospheric Chem Phys 17:14821–14839. https://doi.org/10.5194/acp-17-14821-2017

Feng S, Jiang F, Wang H, Wang H, Ju W, Shen Y, et al (2020) NOx emission changes over China during the COVID-19 epidemic inferred from surface NO2 observations Geophys Res Lett 47https://doi.org/10.1029/2020GL090080

Guan Y, Wang L, Wang S, Zhang Y, Xiao J, Wang X et al (2020) Temporal variations and source apportionment of volatile organic compounds at an urban site in Shijiazhuang, China. J Environ Sci 97:25–34. https://doi.org/10.1016/j.jes.2020.04.022

Hellén H, Tykkä T, Hakola H (2012) Importance of monoterpenes and isoprene in urban air in northern Europe. Atmos Environ 59:59–66. https://doi.org/10.1016/j.atmosenv.2012.04.049

Hui L, Liu X, Tan Q, Feng M, An J, Qu Y et al (2018) Characteristics, source apportionment and contribution of VOCs to ozone formation in Wuhan, Central China. Atmos Environ 192:55–71. https://doi.org/10.1016/j.atmosenv.2018.08.042

Kong SF, Li L, Li XX, Yin Y, Chen K, Liu DT et al (2015) The impacts of firework burning at the Chinese Spring Festival on air quality: insights of tracers, source evolution and aging processes. Atmospheric Chem Phys 15:2167–2184. https://doi.org/10.5194/acp-15-2167-2015

Lal P, Kumar A, Kumar S, Kumari S, Saikia P, Dayanandan A et al (2020) The dark cloud with a silver lining: assessing the impact of the SARS COVID-19 pandemic on the global environment. Sci Total Environ 732:139297. https://doi.org/10.1016/j.scitotenv.2020.139297

Lau AKH, Yuan Z, Yu JZ, Louie PKK (2010) Source apportionment of ambient volatile organic compounds in Hong Kong. Sci Total Environ 408:4138–4149. https://doi.org/10.1016/j.scitotenv.2010.05.025

Li M, Liu H, Geng G, Hong C, Liu F, Song Y et al (2017) Anthropogenic emission inventories in China: a review. Natl Sci Rev 4:834–866. https://doi.org/10.1093/nsr/nwx150

Li L, Li Q, Huang L, Wang Q, Zhu A, Xu J et al (2020) Air quality changes during the COVID-19 lockdown over the Yangtze River Delta Region: an insight into the impact of human activity pattern changes on air pollution variation. Sci Total Environ 732:139282. https://doi.org/10.1016/j.scitotenv.2020.139282

Li M, Wang T, Xie M, Li S, Zhuang B, Fu Q et al (2021) Drivers for the poor air quality conditions in North China Plain during the COVID-19 outbreak. Atmos Environ 246:118103. https://doi.org/10.1016/j.atmosenv.2020.118103

Liu Y, Shao M, Fu L, Lu S, Zeng L, Tang D (2008) Source profiles of volatile organic compounds (VOCs) measured in China: part I. Atmos Environ 42:6247–6260. https://doi.org/10.1016/j.atmosenv.2008.01.070

Liu B, Cheng Y, Zhou M, Liang D, Dai Q, Wang L et al (2018) Effectiveness evaluation of temporary emission control action in 2016 in winter in Shijiazhuang, China. Atmospheric Chem Phys 18:7019–7039. https://doi.org/10.5194/acp-18-7019-2018

Liu Y, Zhong C, Peng J, Wang T, Wu L, Chen Q et al (2022) Evaporative emission from China 5 and China 6 gasoline vehicles: emission factors, profiles and future perspective. J Clean Prod 331:129861. https://doi.org/10.1016/j.jclepro.2021.129861

Mahato S, Pal S, Ghosh KG (2020) Effect of lockdown amid COVID-19 pandemic on air quality of the megacity Delhi, India. Sci Total Environ 730:139086. https://doi.org/10.1016/j.scitotenv.2020.139086

Ministry of Ecology and Environment of the People's Republic of China (2021a) The Ministry of Ecology and Environment released a summary of China's ecological and environmental quality in 2020. Accessed 14/06/2022. Downloaded 14/06/2022. https://www.mee.gov.cn/xxgk2018/xxgk/xxgk15/2021a03/t2021a0302_823100.html

Ministry of Ecology and Environment of the People's Republic of China (2021b) China Ecological Environment Bulletin in 2020. Accessed 14/06/2022. Downloaded 14/06/2022. https://www.mee.gov.cn/hjzl/sthjzk/zghjzkgb/2021b05/P020210b0526572756184785.pdf

NASA (2020) Airborne nitrogen dioxide plummets over China. Accessed 14/06/2022. Downloaded 14/06/2022. https://earthobservatory.nasa.gov/images/146362/airborne-nitrogen-dioxide-plummets-over-china

Paatero P, Tapper U (1994) Positive matrix factorization: a non-negative factor model with optimal utilization of error estimates of data values. Environmetrics 5:111–126. https://doi.org/10.1002/env.3170050203

Pei Z, Han G, Ma X, Su H, Gong W (2020) Response of major air pollutants to COVID-19 lockdowns in China. Sci Total Environ 743:140879. https://doi.org/10.1016/j.scitotenv.2020.140879

Pei C, Yang W, Zhang Y, Song W, Xiao S, Wang J et al (2022) Decrease in ambient volatile organic compounds during the COVID-19 lockdown period in the Pearl River Delta region, south China. Sci Total Environ 823:153720. https://doi.org/10.1016/j.scitotenv.2022.153720

Peng W, Wang Y, Gao X, Jia S, Xu X, Cheng H, et al (2016) Characteristics of ambient formaldehyde at two rural sites in the North

China Plain in summer. Res Environ Sci 29, 1119–1127. https://www.cnki.net/kcms/doi/10.13198/j.issn.1001-6929.2016.08.03.html

Polissar A (1999) The aerosol at Barrow, Alaska: long-term trends and source locations. Atmos Environ 33:2441–2458. https://doi.org/10.1016/S1352-2310(98)00423-3

Polissar AV, Hopke PK, Paatero P, Malm WC, Sisler JF (1998) Atmospheric aerosol over Alaska: 2. Elemental composition and sources. J Geophys Res Atmospheres 103:19045–19057. https://doi.org/10.1029/98JD01212

Reff A, Eberly SI, Bhave PV (2007) Receptor modeling of ambient particulate matter data using positive matrix factorization: review of existing methods. J Air Waste Manag Assoc 57:146–154. https://doi.org/10.1080/10473289.2007.10465319

Sarkar C, Sinha V, Sinha B, Panday AK, Rupakheti M, Lawrence MG (2017) Source apportionment of NMVOCs in the Kathmandu Valley during the SusKat-ABC international field campaign using positive matrix factorization. Atmospheric Chem Phys 17:8129–8156. https://doi.org/10.5194/acp-17-8129-2017

Sbai SE, Mejjad N, Norelyaqine A, Bentayeb F (2021) Air quality change during the COVID-19 pandemic lockdown over the Auvergne-Rhône-Alpes region, France. Air Qual Atmosphere Health 14:617–628. https://doi.org/10.1007/s11869-020-00965-w

Selvam S, Muthukumar P, Venkatramanan S, Roy PD, Manikanda Bharath K, Jesuraja K (2020) SARS-CoV-2 pandemic lockdown: effects on air quality in the industrialized Gujarat state of India. Sci Total Environ 737:140391. https://doi.org/10.1016/j.scitotenv.2020.140391

Shi J, Deng H, Bai Z, Kong S, Wang X, Hao J et al (2015) Emission and profile characteristic of volatile organic compounds emitted from coke production, iron smelt, heating station and power plant in Liaoning Province, China. Sci Total Environ 515–516:101–108. https://doi.org/10.1016/j.scitotenv.2015.02.034

Shijiazhuang Bureau of Statistics (2021) Main economic indicators of the city from January to February 2021. Downloaded 14/06/2022. http://tjj.sjz.gov.cn/col/1584345166496/2021/03/31/1617179498712.html

Sicard P, De Marco A, Agathokleous E, Feng Z, Xu X, Paoletti E et al (2020) Amplified ozone pollution in cities during the COVID-19 lockdown. Sci Total Environ 735:139542. https://doi.org/10.1016/j.scitotenv.2020.139542

Sulaymon ID, Zhang Y, Hopke PK, Zhang Y, Hua J, Mei X (2021) COVID-19 pandemic in Wuhan: ambient air quality and the relationships between criteria air pollutants and meteorological variables before, during, and after lockdown. Atmospheric Res 250:105362. https://doi.org/10.1016/j.atmosres.2020.105362

Tonnesen GS, Dennis RL (2000) Analysis of radical propagation efficiency to assess ozone sensitivity to hydrocarbons and NOx :2. Long-lived species as indicators of ozone concentration sensitivity. J Geophys Res Atmospheres 105:9227–9241. https://doi.org/10.1029/1999JD900372

Tsai SM, Zhang J (Jim), Smith KR, Ma Y, Rasmussen RA, Khalil MAK (2003) Characterization of non-methane hydrocarbons emitted from various cookstoves used in China. Environ Sci Technol 37:2869–2877. https://doi.org/10.1021/es026232a

Vega E, Mugica V, Carmona R, Valencia E (2000) Hydrocarbon source apportionment in Mexico City using the chemical mass balance receptor model. Atmos Environ 34:4121–4129. https://doi.org/10.1016/S1352-2310(99)00496-3

Wang S, Wei W, Du L, Li G, Hao J (2009) Characteristics of gaseous pollutants from biofuel-stoves in rural China. Atmos Environ 43:4148–4154. https://doi.org/10.1016/j.atmosenv.2009.05.040

Wang Y, Yuan Y, Wang Q, Liu C, Zhi Q, Cao J (2020) Changes in air quality related to the control of coronavirus in China: implications for traffic and industrial emissions. Sci Total Environ 731:139133. https://doi.org/10.1016/j.scitotenv.2020.139133

Xuan L, Ma Y, Xing Y, Meng Q, Song J, Chen T et al (2021) Source, temporal variation and health risk of volatile organic compounds (VOCs) from urban traffic in Harbin, China. Environ Pollut 270:116074. https://doi.org/10.1016/j.envpol.2020.116074

Yuan B, Shao M, Lu S, Wang B (2010) Source profiles of volatile organic compounds associated with solvent use in Beijing, China. Atmos Environ 44:1919–1926. https://doi.org/10.1016/j.atmosenv.2010.02.014

Zhang Y (2020) Study on the characteristics of ozone pollution and its relationship with precursors in piedmont cities in Hebei. Hebei Univ Sci Technol. https://doi.org/10.27107/d.cnki.ghbku.2020.000464

Zhang Y, Wang X, Zhang Z, Lü S, Shao M, Lee FSC, Yu J (2013) Species profiles and normalized reactivity of volatile organic compounds from gasoline evaporation in China. Atmos Environ 79:110–118. https://doi.org/10.1016/j.atmosenv.2013.06.029

Zhang J, Yang L, Chen J, Mellouki A, Jiang P, Gao Y et al (2017) Influence of fireworks displays on the chemical characteristics of PM2.5 in rural and suburban areas in Central and East China. Sci Total Environ 578:476–484. https://doi.org/10.1016/j.scitotenv.2016.10.212

Zhang Y, Xue L, Carter W, Pei C, Chen T, Mu J et al (2021) Development of ozone reactivity scales for volatile organic compounds in a Chinese megacity. Atmospheric Chem Phys 21:11053–11068. https://doi.org/10.5194/acp-2021-44